Impacts of Land Surface Model Complexity on a Regional Simulation of a Tropical Synoptic Event

H. ZHANG

Bureau of Meteorology Research Center, Melbourne, Australia

J. L. MCGREGOR

CSIRO Atmospheric Research, Melbourne, Australia

A. HENDERSON-SELLERS

Environment Division, Australian Nuclear Science and Technology Organisation, Sydney, Australia

J. J. KATZFEY

CSIRO Atmospheric Research, Melbourne, Australia

(Manuscript received 15 October 2002, in final form 4 August 2003)

ABSTRACT

A multimode Chameleon Surface Model (CHASM) with different levels of complexity in parameterizing surface energy balance is coupled to a limited-area model (DARLAM) to investigate the impacts of complexity in land surface representations on the model simulation of a tropical synoptic event. A low pressure system is examined in two sets of numerical experiments to discuss the following. (i) Does land surface parameterization influence regional numerical weather simulations? (ii) Can the complexity of land surface schemes in numerical models be represented by parameter tuning? The model-simulated tracks of the low pressure center do not, overall, show large sensitivity to the different CHASM modes coupled to the limited-area model. However, the landing position of the system, as one measurement of the track difference, can be influenced by several degrees in latitude and about one degree in longitude. Some of the track differences are larger than the intrinsic numerical noise in the model estimated from two sets of random perturbation runs. In addition, the landing time of the low pressure system can differ by about 14 h. The differences in the model-simulated central pressure exceed the model intrinsic numerical noise and such variations consistent with the differences seen in simulated surface fluxes. Furthermore, different complexity in the land surface scheme can significantly affect the model rainfall and temperature simulations associated with the low center, with differences in rainfall up to 20 mm day^{-1} and in surface temperature up to 2°C. Explicitly representing surface resistance and bare ground evaporation components in CHASM produces the most significant impacts on the surface processes. Results from the second set of experiments, in which the CHASM modes are calibrated by parameter tuning, demonstrate that the effects of the physical processes represented by extra complexity in some CHASM modes cannot be substituted for by parameter tuning in simplified land surface schemes.

1. Introduction

Assessing the sensitivity of numerical models to the representation of land surface processes has been, and continues to be, an important scientific issue in numerical weather and climate forecasts. The importance of land surface processes arises because of the large energy and water exchange at the continental surface and the complexity of interactions between the land surface and the overlying atmosphere. Land surface, as part of the lower boundary of the atmosphere, determines how radiative energy (shortwave and longwave) arriving at the land surface is partitioned into latent and sensible heat fluxes and how water reaching the land surface becomes soil water storage, runoff, and drainage and how much water is recycled into the atmosphere. These heat and water fluxes are important in determining the dynamical and physical processes in the overlying atmosphere.

The complexity of land surface models has tended to grow as our knowledge of land surface processes has increased and our appreciation of the importance of land surface processes in the weather and climate system has developed. Land surface schemes have evolved from

Corresponding author address: Dr. Huqiang Zhang, Bureau of Meteorology Research Center, GPO Box 1289K, Melbourne, VIC 3001, Australia.
E-mail: h.zhang@bom.gov.au

simple bucket-type models (Manabe 1969) into complex soil–vegetation–atmosphere transfer schemes (e.g., Dickinson et al. 1986; Sellers et al. 1986; Henderson-Sellers et al. 2003). Now, the inclusions of carbon cycle and interactive vegetation are becoming intense research areas in the land surface and climate modeling community (e.g., Sellers et al. 1997; Cox et al. 1999). The variation of complexity in land surface models currently used in weather and climate numerical models is immense. This happens because of different philosophies used in developing surface schemes (Shao and Henderson-Sellers 1996; Sellers et al. 1997); different model structures used in building the schemes (Henderson-Sellers 1996) and even different effective meaning of parameters used in the models (Desborough 1997; Wood et al. 1998; Irannejad et al. 2003). Results from the Project for Intercomparison of Land Surface Parameterization Schemes (PILPS; e.g., Henderson-Sellers et al. 1995, see special issue of *Global and Planetary Change,* 1998, Vol. 9) have revealed poor agreement among current land surface schemes in representing key surface processes such as surface water and energy partitioning when forced with the same meteorological forcing.

Three questions then arise: (i) do land surface processes matter in the numerical model simulations of weather and climate? Then, if assured in the affirmative, (ii) how complex should land surface schemes be in current numerical models, particularly when considering that the representations of known important atmospheric processes such as convection and clouds in numerical models are still simple compared with reality? and (iii) can such complexity be represented by parameter tuning? Zhang et al. (2001b), by coupling a multiple-complexity-mode land surface scheme with a regional climate model, tried to address some of the issues on land surface modeling and climate simulations.

In this study, we report a similar study to that of Zhang et al. (2001b), but with a focus on simulating a specific synoptic weather event. In particular, by coupling a multimode land surface scheme, which has different levels of complexity in solving the surface energy balance, to a limited-area model, we try to explore the impacts of complexity in land surface parameterization in simulating deep synoptic weather events. Previous studies (e.g., Timbal and Henderson-Sellers 1998; Hopkins and Henderson-Sellers 1999) showed a regional numerical model's sensitivity to land surface processes. Nevertheless, because two or more, completely different land surface schemes were employed in such studies, it was difficult to conclude what part of the land surface representation was causing the model's sensitivity: complexity, structure, or even parameter values. When the features of the multimode land surface scheme used in this study are described later, one can see the advantage of the approaches in the current study and how it differs from the previous ones in assessing relationships between complexity in land surface schemes and weather simulations.

Another issue to be discussed in this study is: can extra complexity in the surface representation be substituted by parameter tuning? For instance, the old version of the UK Met Office (UKMO) surface scheme (Warrilow et al. 1986) implicitly combined the contribution of dry vegetation and bare ground evaporation into a single geographic variable, surface resistance, to calculate the combined surface fluxes. Similarly, McFarlane et al. (1992) implemented a variable bucket surface scheme in a GCM in which surface water field capacity varied with location to try to account for the effects of the vegetation contribution to surface evaporation. With concerns over computational efficiency in operational numerical weather forecasts and long-term climate simulations, as well as the demand of developing simplified models in helping us understand the complicated physical and dynamical processes in weather and climate forecasts, the issue of the complexity of weather and climate numerical models still draws further studies in the research community. Zhang et al. (2001b) tackled this issue in the context of regional climate simulation and showed that the contribution from physical processes represented by the extra complexities in land surface schemes cannot be represented by tuning some parameters in simplified schemes. The same issue will be pursued further in the context of numerical weather modeling.

This paper is structured as follows. In section 2, we briefly describe the limited-area model used in the study and the multimode land surface scheme coupled to the limited-area model. Section 3 describes the synoptic events and the numerical experiments we conducted. Section 4 shows the regional model's overall sensitivity to different complexity in land surface representations and section 5 discusses whether tuning parameters in simple land surface models can represent the contribution from extra complexity in more complex land surface models. Conclusions drawn from this study and discussions are presented in section 6.

2. Model description

As in Zhang et al. (2001b), the Australian Commonwealth Scientific and Industrial Research Organization (CSIRO) Division of Atmospheric Research Limited-Area Model (DARLAM; McGregor 1987; Walsh and McGregor 1995) is used in this study. This model has been used for both synoptic and regional climate simulations (Evans et al. 1994; Walsh and McGregor 1995; Walsh and Watterson 1997) and climate change studies (Walsh and Katzfey 2000). DARLAM is a two-time-level, semi-implicit hydrostatic primitive equation model, uses a staggered Arakawa C grid with a Lambert conformal projection and applies semi-Lagrangian horizontal advection with bicubic spatial interpolation. In the current study, 75-km resolution is used over a do-

TABLE 1. The configuration of surface energy balance in the CHASM modes (adapted from Desborough 1999).

CHASM mode	Stability correction	Surface resistance	Canopy interception	Bare ground evaporation	Canopy resistance	Temperature differentiation
EB	Yes	No	No	No	No	No
RS	Yes	Yes	No	No	No	No
RSI	Yes	Yes	Yes	No	No	No
RSGI	Yes	Yes	Yes	Yes	No	No
SLAM1	Yes	Yes	Yes	Yes	Yes	No
SLAM	Yes	Yes	Yes	Yes	Yes	Yes

main approximately from 60° to 5°S and from 65° to 195°E. There are 18 vertical levels in the model configuration. The Arakawa–Gordon cumulus convection scheme, described by McGregor et al. (1993), is applied in this study. The model is run with a 9-min time step and the nesting data are derived from the National Centers for Environmental Prediction–National Center for Atmospheric Research (NCEP–NCAR) reanalysis data of Kalnay et al. (1996). At each time step, the outermost boundary rows of DARLAM are relaxed toward the interpolated values provided every 6 h from the reanalysis data, using the one-way nesting procedure of Davies (1976).

The version of the multimode Chameleon Surface Model (CHASM) in this study is identical to that described in Desborough (1999) and used in Zhang et al. (2001b), Xia et al. (2002), and Pitman et al. (2003). There are six different modes in CHASM. As summarized in Table 1, the simplest mode (EB) is a Manabe-type bucket scheme with a single surface energy balance, single evaporation flux, and no surface resistance. The most complex mode (SLAM) is a mosaic-type scheme in which the land–atmosphere interface is divided into two tiles: the first presenting a combination of bare ground and exposed snow to the atmosphere and the second consisting of vegetation. This mode has explicit parameterizations for canopy resistance, canopy interceptions, and bare ground evaporation.

There are four intermediate surface energy configuration modes in CHASM: the RS mode includes temporally invariant surface resistance (r_s) to the pathway of snow-free evaporation; the RSI mode explicitly adds canopy interception to the RS mode; the RSGI mode explicitly incorporates bare ground evaporation into the RSI mode; and the last intermediate mode (named SLAM1) is a one-tile version of SLAM where a single surface energy balance expression is resolved. Intermediate complexity modes RS, RSI, RSGI, and SLAM1 in CHASM are constructed around a surface resistance component, which represents the influences of canopy stomatal stresses on transpiration other than moisture availability. Surface resistance is prescribed in RS, RSI, and RSGI modes, while in SLAM1 and SLAM it is calculated as a function of radiation, temperature, and humidity. By choosing r_s values through offline calibration (described in section 3), CHASM becomes a fully controlled tool such that all of its surface energy balance configurations use the same effective parameterizations and parameters (Desborough 1999). Each surface energy balance mode is combined with a common hydrological module based on Manabe (1969). All modes share a common six-layer soil temperature module (Desborough 1999).

Therefore, by coupling CHASM with DARLAM, we can isolate factors such as different model structures and different effective meanings of parameters in explaining the model results. The only factors contributing to the differences (if any) in coupled experiments are the different model complexities in land surface representations. This feature makes the current study different from the ones mentioned in the introduction.

3. Description of the synoptic case and numerical experiments

Previous studies tended to suggest that the importance of land surface processes becomes clear when the simulated weather system is shallow (e.g., Hopkins et al. 1999). However, Zhang et al. (2001b) found that the track of a tropical-cyclone-like feature in the period of their studies was affected by the complexity in the CHASM modes. In this study, we chose the synoptic event associated with Tropical Cyclone Vance as our case study. It must be emphasized here that our current study is not directed to how tropical-cyclone-like vortices are simulated in the limited-area model, or how tropical cyclone forecasts are affected by land surface schemes. This is because to simulate tropical cyclones (TCs) in numerical models realistically, one needs a high-resolution model and specific approaches in data assimilation and initialization such as the ''bogusing'' technique (e.g., Serrano and Unden 1994; Davidson and Weber 2000). In this study, the model resolution is only 75 km and no bogusing or sophisticated model initialization and data assimilation is considered. In the analysis, we only focus on exploring the model sensitivity to different complexity in the CHASM modes in its simulation of synoptic aspects associated with the cyclone activity. Validating the model simulation against observations is not our primary goal, although better understanding of the model sensitivity to its physical parameterizations will eventually help us to improve the model forecasts against observations.

Figure 1 shows the synoptic history of the low pres-

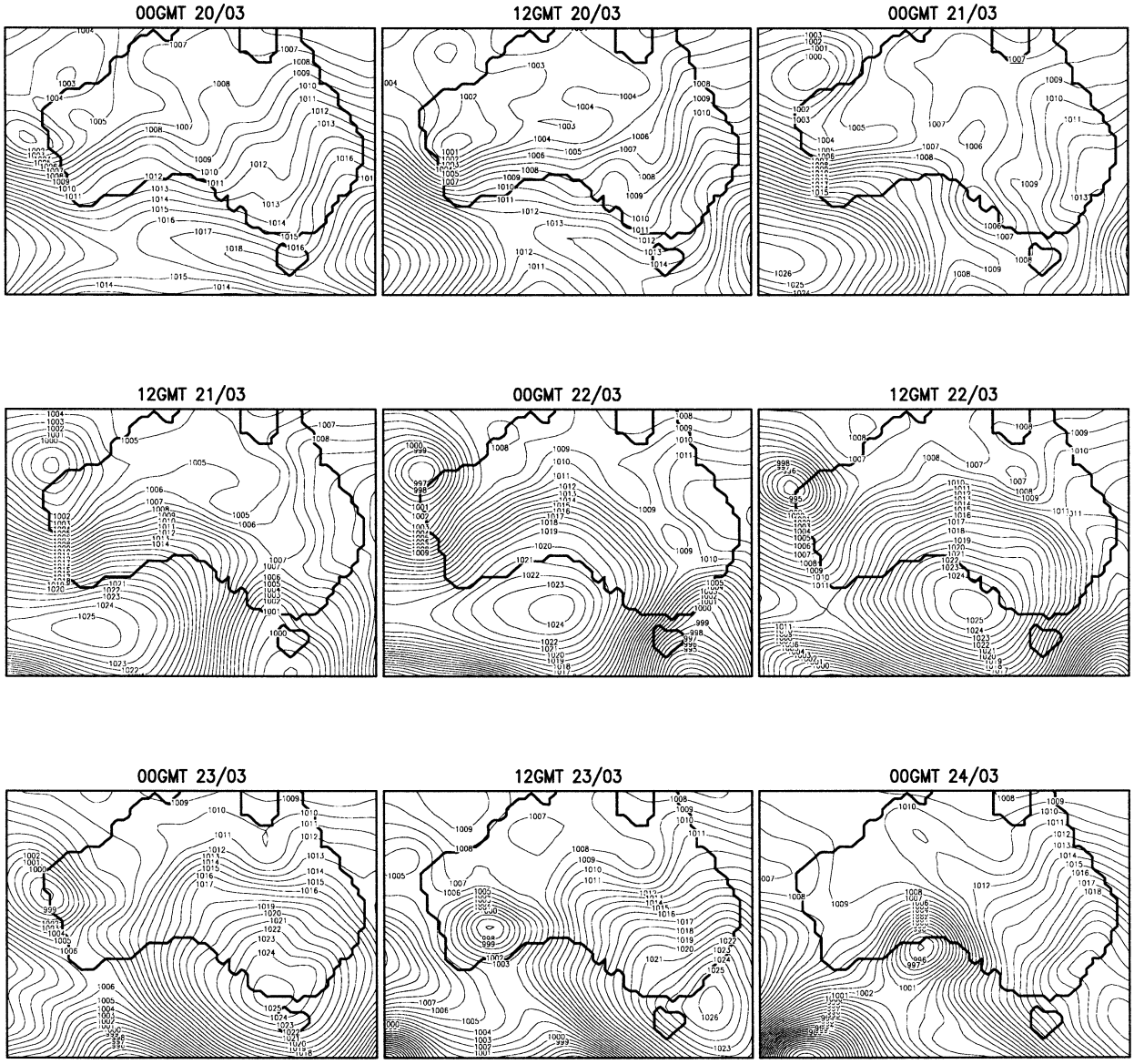

FIG. 1. Mean sea level pressure (hPa) from the nesting data derived from the NCEP–NCAR reanalysis data of Kalnay et al. (1996).

sure system associated with TC Vance from the nesting dataset as presented in the mean sea level pressure (MSLP) for the period of 20–24 March 1999. The low pressure centers in the nesting data are much weaker than observed (see details online at http://www.bom.gov.au/info/cyclone/vance/vance.shtml) for TC Vance, which was classified as a category-5 severe tropical cyclone overnight on 21 March. In the nesting data, only after 22 March did the central pressure become less than 1000 hPa. This is likely to be due to the coarse resolution in the numerical model used in generating the reanalysis data, the 2.5° × 2.5° resolution of the reanalysis output where extreme values are likely to be smoothed, and lack of observational data to define the inner core. With such a weak disturbance in the nesting data, one cannot expect the limited-area model to generate realistic cyclone intensities in its simulations. Bearing in mind that the main motivation of this study is to assess how different complexity in land surface schemes can affect the model forecasts of a severe weather event, we are more interested in exploring and understanding the differences between the DARLAM simulations of the synoptic features associated with the cyclone using different CHASM modes, rather than contrasting in detail the simulations with observations. Thus, such deficiencies in the initial data do not negate the value of the study.

In this study, we mainly report results by initializing the model with data from 0000 UTC 20 March 1999. In addition, we conducted a set of complementary experiments by initializing the model with data from 0000

UTC 22 March 1999 when the central pressure was below 997 hPa in the nesting data (Fig. 1). We found that DARLAM was then able to simulate low pressure centers with central pressure below 995 hPa. As the scientific conclusions from the complementary experiment are similar to the runs starting from 20 March, detailed analysis of the results starting from the 22 March runs will not be presented in this paper. To isolate the impacts of different land surface initial conditions on the model simulation and taking advantage of CHASM's structure that all its modes share the same soil temperature and moisture module, all the experiments in this study use the same soil temperature and soil moisture initial conditions as derived from the reanalysis datasets. The bucket initial soil moisture is set as the soil moisture (fraction) at the layer of 10–200 cm derived from the reanalysis. Similarly, initial deep soil temperatures in CHASM (layers 3–6) are set as the low-level soil temperature from the reanalysis, and the initial temperatures of the upper two layers are set to the skin temperature from the reanalysis. Certainly, different initial conditions can produce significant impacts on the regional model simulations, as noted by Nagata et al. (2001), and allowing soil moisture spinup could affect the model simulations and the model sensitivity results. There are studies on how to better initialize weather forecasting models and how to better design initial perturbations to form ensemble forecasts. However, this is out of the scope of this study although it shall be pursued in future investigations.

Desborough (1999) showed that the scatter of the partition of surface energy simulated by different CHASM modes was similar to that found in the PILPS offline experiments. Therefore, we first couple the six CHASM modes, which broadly capture the scatter seen in most land surface schemes currently being used in weather and climate simulations, to DARLAM to assess overall whether the simulated weather events are affected by different surface model complexity. Based on the experiments conducted by Zhang et al. (2001b), we use the surface resistance r_s values as 50, 80, and 150 s m^{-1} for the RS, RSI, and RSGI modes, respectively.

When assessing DARLAM's sensitivity to different complexity modes in CHASM, it is very desirable to estimate the model's intrinsic numerical noise in order to make valid conclusions on whether the host model is affected by different surface representations. As in Zhang et al. (2001b), we have conducted 10 DARLAM perturbation runs with the EB mode by randomly disturbing the lowest level air temperature by ± 0.1°C in the model initial condition over the whole model domain. We have also performed five perturbation runs using the SLAM mode. Thus, by contrasting the model sensitivities to different CHASM modes to the model internal numerical noises derived from the perturbation runs, it allows us to assess whether such model sensitivities are numerical noise or the impacts from land surface processes. Note that the spread seen from the perturbation runs could be different by projecting the perturbation in the direction of the model's singular vectors as used in operational weather forecasts (e.g., Molteni et al. 1996). However, it needs to be pointed out that the purpose of such perturbation runs is not aimed at forming ensemble predictions, rather it is merely to estimate the sensitivity to numerical noise in the model. In addition, as generally known to the numerical weather forecasting community (e.g., Nagata et al. 2001), short-term numerical weather forecasts are very sensitive to initial conditions. Therefore, imposing larger perturbations in the model initial condition could mask the signals from the changes of the model physics. This is the reason why we have chosen a small magnitude in the perturbation runs.

As in Zhang et al. (2001b), our second set of experiments is designed such that we first conduct a set of offline experiments to choose different r_s values for the three intermediate CHASM modes (RS, RSI, and RSGI), so that they give similar surface energy partitions to those from SLAM1 (surface resistance is calculated in SLAM1) with the same meteorological forcing. Then, we focus on the analysis of coupled model results in which the r_s value over each land grid point is obtained from the offline calibration. These analyses examine whether different complexity in the CHASM modes affects the model simulation in the coupled environment, even after selection, to have similar features in offline simulations. It also helps us to answer the question: can the effective contribution from extra complexities in land surface schemes be represented by adjusting tunable parameters in the surface model itself?

4. Model sensitivity to different complexity in surface representation

In this section, we present results from experiments coupling DARLAM with six CHASM modes without any calibration. By initializing DARLAM with the nesting data at 0000 UTC 20 March 1999, a 5-day model integration is conducted for each of the six CHASM modes. Surface resistance (r_s), the key parameter in the CHASM modes, is prescribed as 50, 80, 150 s m^{-1} in the RS, RSI, and RSGI modes. As described in section 2, there is no surface resistance component in the bucket EB mode and surface resistance is calculated in the SLAM1 and SLAM mode as a function of radiation, humidity, and temperature (Desborough 1999). Thus, results presented here demonstrate DARLAM's overall sensitivity to the CHASM modes, which have a similar scatter to that seen in current land surface schemes in the PILPS project.

In the analysis of the model results, we simply use the model-simulated MSLP in positioning the low pressure centers and use it in estimating the cyclone strength. The accuracy of using MSLP in positioning tropical cyclones before its circulation becomes vertically organized has been questioned by the tropical cyclone

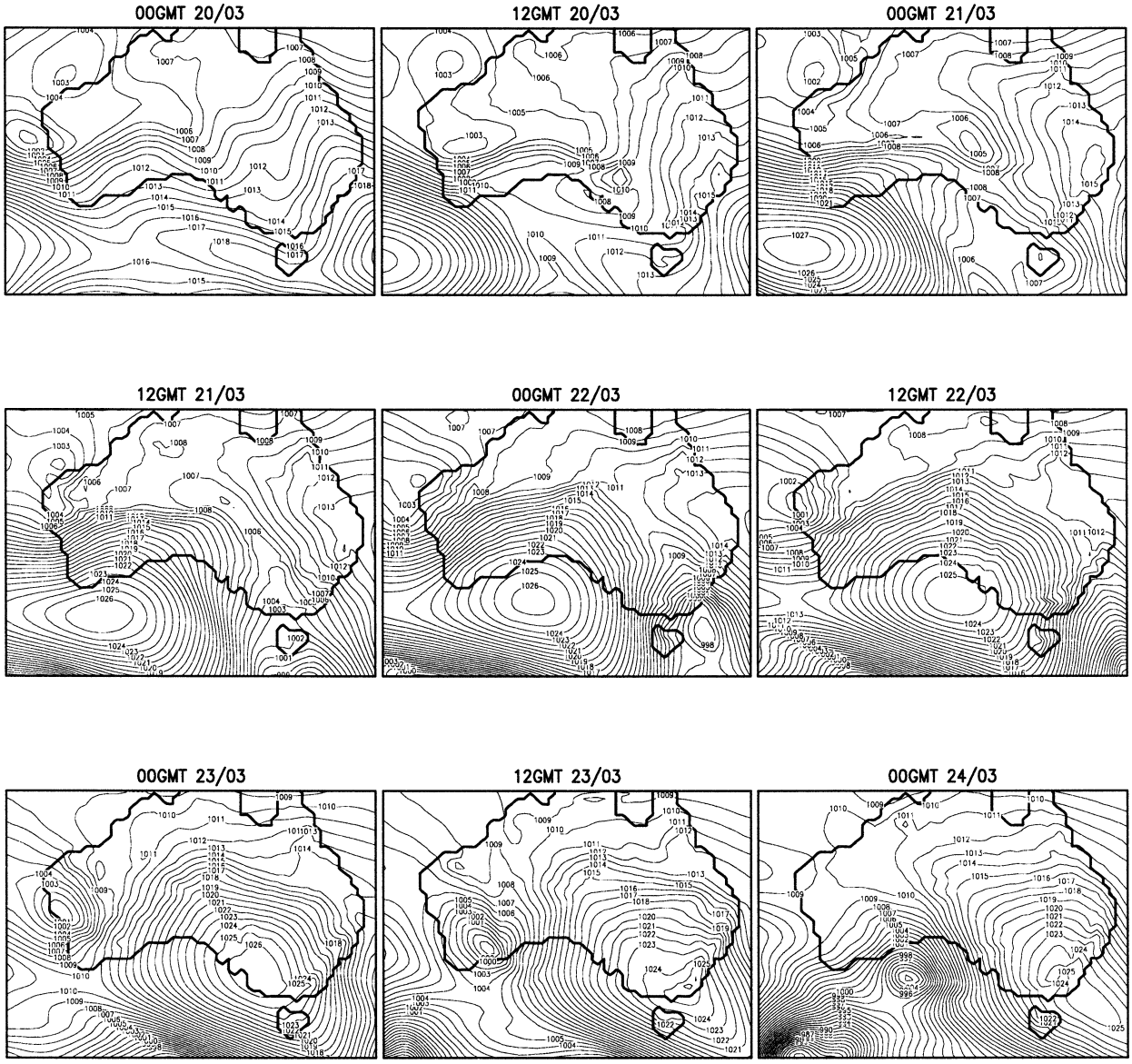

FIG. 2. Time slices of simulated mean sea level pressure from DARLAM coupled with CHASM's EB mode for the period 20–24 Mar 1999. The model is initialized at 0000 UTC 20 Mar 1999.

research community, but it is not an issue here as we only concentrate on exploring the differences due to different land surface models employed in forecasting the movement of the low pressure center. Figure 2 shows time slices of the simulated mean sea level pressure for the period 20–24 March. Comparing these with the synoptic patterns seen in Fig. 1, we see that DARLAM is able to reproduce the movement of the low pressure center, as well as the overall large-scale pressure pattern of the reanalysis data. However, the intensity of the low center is much weaker than that seen in Fig. 1. This is largely due to the low resolution of the model and a very weak disturbance in the initial nesting data. As the low pressure system simulated in the model is much weaker than observed, impacts from different CHASM modes in the cyclone activity could be different if the simulated system has more realistic features. Thus, in this study we limit our focus on assessing whether the model's simulations of the synoptic low pressure center are sensitive to different complexity in CHASM modes, without making a definitive conclusion on the potential impacts of land surface modeling on severe tropical cyclones.

To explore the model's sensitivity to the six CHASM modes, Fig. 3 displays the model-simulated low pressure tracks for the period 1600 UTC 20 March to 0400 UTC 24 March from each of the model runs. The paths of the low pressure center from each of the DARLAM

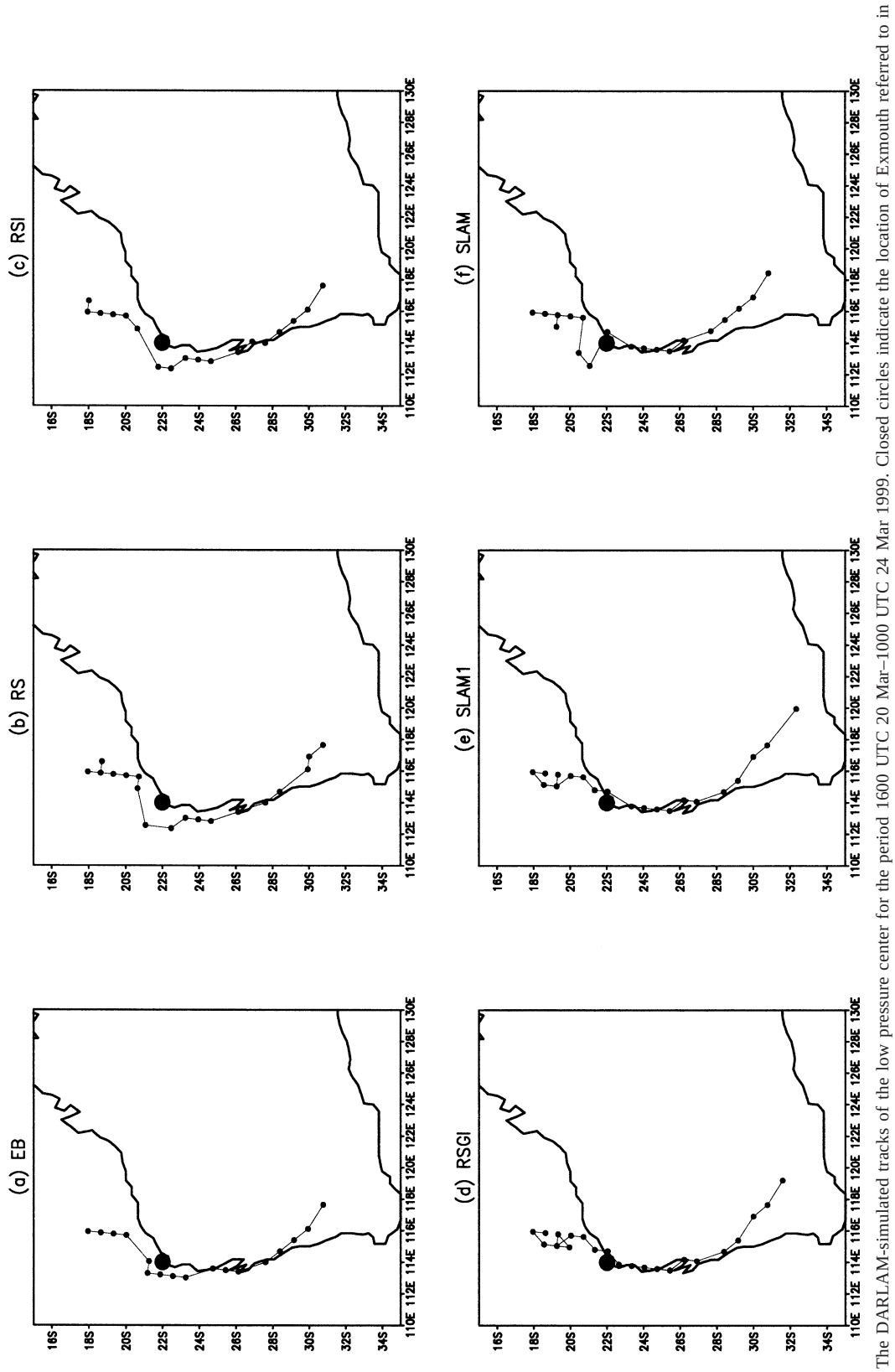

FIG. 3. The DARLAM-simulated tracks of the low pressure center for the period 1600 UTC 20 Mar–1000 UTC 24 Mar 1999. Closed circles indicate the location of Exmouth referred to in Fig. 9.

TABLE 2. The landing time of the low pressure system simulated by the six DARLAM runs.

Mode	EB	RS	RSI	RSGI	SLAM1	SLAM
Landing time	1424 UTC 22 Mar	1912 UTC 22 Mar	1912 UTC 22 Mar	0448 UTC 22 Mar	0448 UTC 22 Mar	0712 UTC 22 Mar

simulations employing different CHASM modes are similar. In comparison to observations (not shown), the paths of the low pressure center are generally more southward, but with similar positions as seen in the nesting data in Fig. 1. Such results indicate that once the large-scale environment, where the tropical-cyclone-associated disturbance is embedded, is well established in the model initial state, the model-simulated tracks of the low pressure system are, in general, less affected by different land surface representations. Note that TC Vance is a severe tropical storm with a typical track, largely determined by the well-established large-scale environmental flow. Therefore, the role of land surface modeling in such a deep system would be relatively small, as found by Hopkins et al. (1999). If a system is weak and has irregular movement during its life cycle, then the impacts of land surface parameterization could be more significant, as shown in Zhang et al. (2001b). This is one of the issues to be studied further in the future.

Nevertheless, further comparison of the results in Fig. 3 suggests that some of the changes at local or regional scales can be significantly different. For instance, the low center in the run with RS mode has large westward movement and then it progressively moves southward along the coast and makes its first landing near 26.1°S and 113.4°E. In contrast, the low center in the RSGI run has some irregular motions at its early stage and then moves slightly southwestward by making its first landing at roughly 22°S and 114.7°E. There is about a 4° difference in latitude and 1° in longitude, in terms of its first landing position. The impacts of such a difference can be significant in terms of emergency management of potential hazards for the regional community affected (e.g., McGuffie and Zhang 1997). Furthermore, it needs to be pointed out that the model-simulated track difference is the difference of the mean motion of a well-resolved large-scale low pressure system. The track of the system is not determined by details of the inner core alone, which cannot be resolved in the model with its current resolution, but by the large-scale mean circulation.

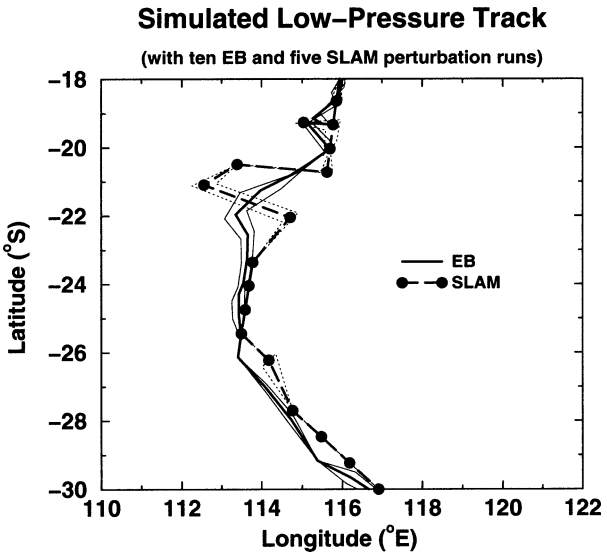

FIG. 4. The DARLAM-simulated tracks of the low pressure center for the period 1200 UTC 21 Mar–0700 UTC 23 Mar 1999 during its landing period (time interval is 144 min). Thick solid line represents the ensemble average of the 10 perturbation runs using the EB mode. Thin solid lines represent the model spread (1 std dev) derived from 10 EB perturbation runs. Thick dashed line with filled circles represents results from the model simulation using the SLAM mode and the thin dashed lines represent the model spread (1 std dev) derived from five SLAM perturbation runs.

In addition to the discussion of the differences between the model-simulated landing positions, which is a useful indicator for showing the impacts of land surface modeling on the local and regional features of the synoptic system, Table 2 summarizes the landing time difference simulated by the six DARLAM experiments. The landing time is estimated from the model outputs, which are saved 10 times per day during the integration. Differences between the low pressure landing time from the six runs are demonstrated in Table 2. The RS and RSI runs simulate the landing time as about 1910 UTC 22 March, while the landing time is simulated as about 0440 UTC 22 March by the RSGI and SLAM1 modes, and 0710 UTC 22 March by the SLAM mode. The largest difference is over 14 h between the RS/RSI mode and the RSGI/SLAM1 mode. Again, such a difference in forecasting the landing time of the system can be important in terms of emergency management in the areas affected. This is another indicator for showing the impacts from land surface modeling.

To further assess whether some of the differences seen in Fig. 3 are the result of the model sensitivity to difference CHASM modes, Fig. 4 contrasts the paths before and after the low pressure system's landing period, simulated by DARLAM coupled with the EB and SLAM modes. The two thin solid lines represent the spread (one standard deviation) of tracks in the 10 perturbation runs using EB mode. Similarly, the two thin dotted lines are from five perturbation runs using SLAM mode. Overall, the spread seen between runs using EB and SLAM modes are larger than the model internal numerical noise. Therefore, although the broad picture

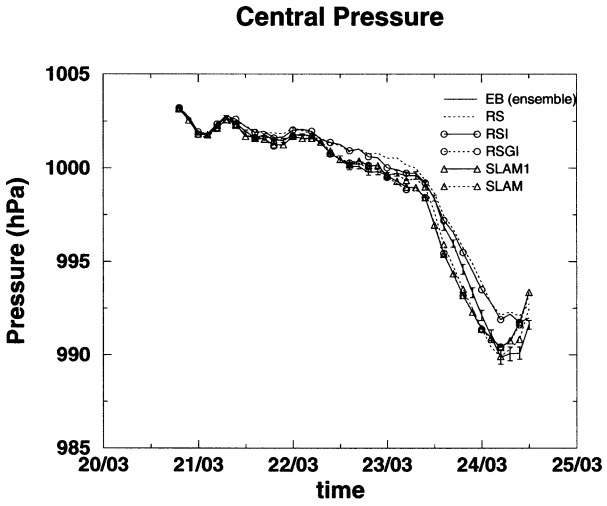

FIG. 5. The DARLAM-simulated central pressure (hPa) of the low center. The period of 22–24 Mar roughly corresponds to its excursion over land. The solid line without symbol represents the ensemble average of the 10 perturbation runs using the EB mode. Error bars attached to the solid line represent the model spread (1 std dev) derived from the 10 perturbation runs.

of the movement of the low pressure center in the model is not dramatically altered (see Fig. 3), results from Fig. 4 demonstrate that the local features can be altered by employing different land surface modes. The simulated track difference is comparable with the standard error in tropical cyclone operational forecasts (e.g., Davidson and Weber 2000). Furthermore, results from Nagata et al. (2001), comparing current mesoscale numerical models in simulating an explosive tropical cyclone's development, showed that enhancing numerical model resolution has little impact on the model track prediction. Thus, results from the current study may not be severely devalued by the model's low resolution. By employing such a multimode land surface scheme, one can obtain an indication of the uncertainty due to the representation of land surface processes in numerical models.

Figure 5 shows the time series of the central pressure of the low center in the six DARLAM integrations with different CHASM modes. Again, results from the 10 perturbation runs are included to help assess the significance of the model results using different CHASM modes. In the simulations, the low pressure center is located over the continent roughly between 0000 UTC 22 March and 0000 UTC 24 March. As noted, the low pressure center is far weaker in the model than in observations and the differences between runs with the various CHASM modes start to occur after its landing. There are central pressure differences of about 2.5 hPa between some of the modes in the period 23–24 March. This is roughly equivalent to a wind speed of 2.1 m s^{-1} according to Atkinson and Holliday (1977). Compared with the averaged absolute wind forecast errors (roughly 5.5 m s^{-1}) from 24-h operational forecasts (Sampson et al. 1995), such discrepancies seen in the DARLAM simulations are small but significant. Figure 5 also demonstrates that most of the differences between runs using different CHASM modes are larger than the error bars seen from the EB perturbation runs, suggesting such differences are primarily due to surface representations, not model internal noise. Further comparison between the changes in the central pressure with the changes in surface fluxes (shown in Fig. 8 and discussed later) suggests that the weaker low pressure system simulated in a number of runs (e.g., RS and RSI) is consistent with the reduction in surface evaporation simulated in these modes (Fig. 8). This is because the weakening of surface moisture supply through surface evaporation prevents the intensification of the low pressure system, as shown in studies of the decay of tropical cyclones over land (e.g., Tuleya 1994).

Associated with the changes in the model simulations of low pressure track and intensity, the model-simulated rainfall intensity and distributions are analyzed. Figure 6 shows the daily accumulated rainfall on 22 and 23 March with different CHASM modes. Again, to assess whether differences between the model runs are from model numerical noise or due to the impacts of different complexity represented in CHASM, regions where the difference is larger than 2 times the standard deviation from the 10 EB perturbation runs are shaded. On 22 March, heavy rainfall is generated by the low pressure center in the western coastal region (Fig. 6a). Progressively increasing the complexity in the CHASM modes leads to changes of rainfall intensity and distribution over the regions influenced by the low pressure center. These changes are the consequence of changes in its track and intensity as discussed before. In addition, moderate changes in daily rainfall are also seen in the eastern continent region (not shown), especially between the RS–EB and RSGI–RSI, emphasizing the influence of introducing a surface resistance component and explicit representation of ground evaporation in the modes. Such results are consistent with the results of Zhang et al. (2001b).

Associated with the land excursion of the low pres-

→

FIG. 6. Comparison of DARLAM-simulated daily accumulative precipitation (mm day^{-1}) on 22 and 23 Mar using different CHASM modes. (a) and (g) The model simulations using the EB mode; the rest are the difference between simulations from two CHASM modes. Contour intervals are −30, −20, −10, −5, and −1 mm day^{-1} for dashed lines and 1, 5, 10, 20, 30 mm day^{-1} for solid lines. Changes within the range of ±1 mm day^{-1} are not shown to keep the diagrams simple. Changes with magnitude larger than twice the standard deviation derived from the 10 EB perturbation runs are shaded. The square area indicated by the heavy dashed lines is the area used in the calculation of Table 2.

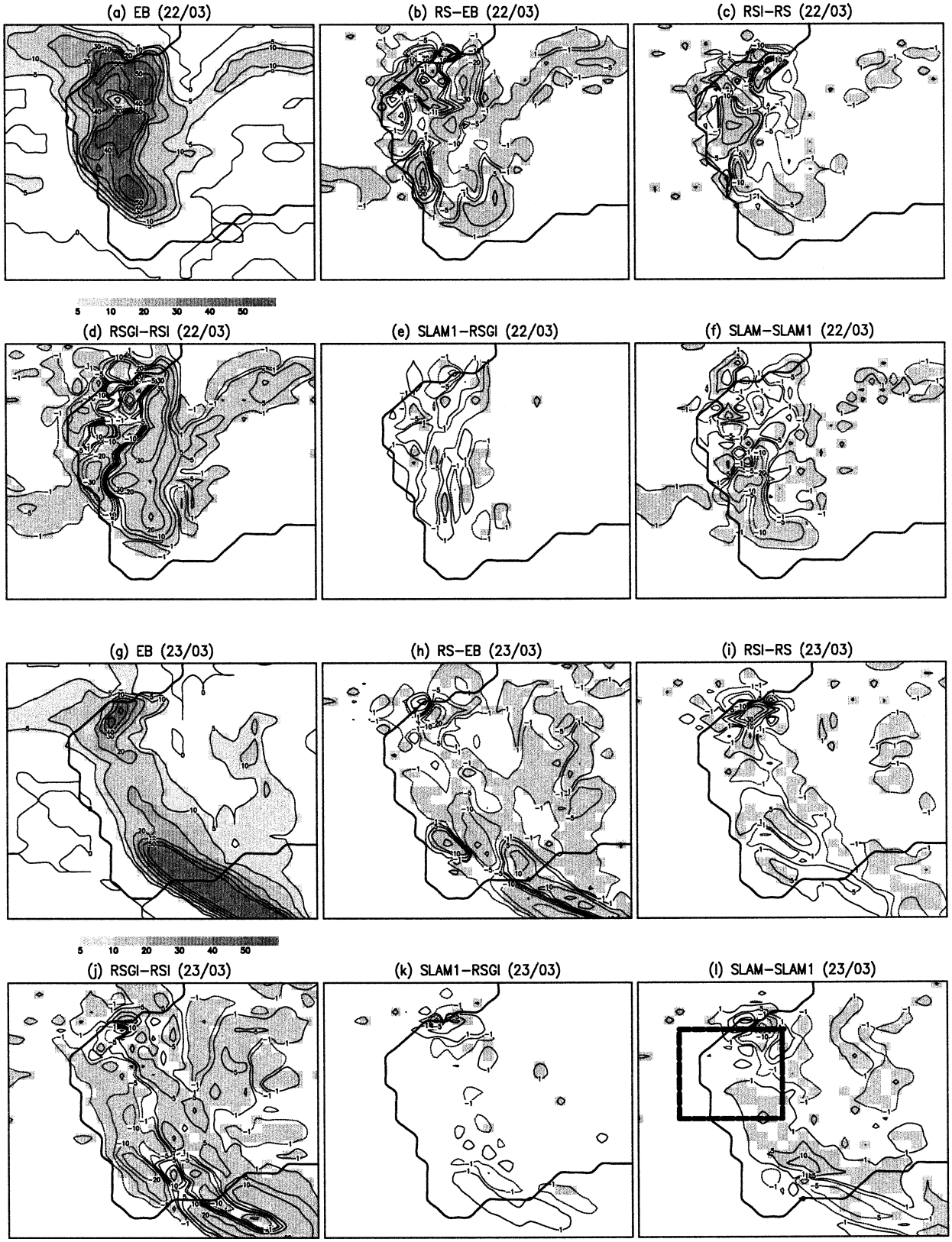

TABLE 3. The areally averaged daily accumulative rainfall (mm day^{-1}) over the land area of 21°–27°S and 110°–120°E from the six DARLAM runs on 22 and 23 Mar. The location of the region is shown in Fig. 61.

	EB	RS	RSI	RSGI	SLAM1	SLAM
22 Mar	39.9	35.5	37.2	41.4	41.4	40.9
23 Mar	15.6	12.1	14.6	13.4	13.7	13.6

sure system, heavy rainfall is simulated along the track of the low center on 23 March (Figs. 6g–i). Similar model sensitivities are seen in the daily rainfall distribution and intensity. Progressively increasing the complexity in the CHASM modes modifies the rainfall intensity and distribution in the cyclone-affected region, as well as in the northern and eastern regions. Again, the most significant changes are seen when surface resistance is introduced in the RS mode and when bare ground evaporation is explicitly represented in the RSGI mode.

To assess if the changes of rainfall seen in Fig. 6 are purely due to the displacement of rainfall patterns because of changes in the low pressure track, areally averaged rainfall is calculated over the land area of 21°–27°S and 110°–120°E for all six runs for 22 and 23 March. The location of the region is shown in Fig. 6I, where heavy rainfall associated with the low pressure center is simulated and where the low center makes its landing in the six runs. Differences are seen in the averaged daily rainfall (Table 3). The RS run has the smallest areally averaged rainfall on both 22 and 23 March. On 22 March, it is 35.5 mm day^{-1} in the RS run, while it is 41.4 mm day^{-1} in the RSGI run. On 23 March, the daily accumulated rainfall is 12.1 mm day^{-1} in the RS run, but it can be as high as 15.6 mm day^{-1} in the EB runs. The reduction of daily rainfall in the RS mode is consistent with the significant decrease in surface evaporation (see Fig. 8). It is possible that the uniformly reduced surface evaporation in the RS mode (Fig. 8b), as part of the atmospheric moisture source through surface water recycling, makes part of the contribution to the decreased rainfall. As a positive feedback, the reduction of rainfall can further lead to the decrease of surface evaporation.

Figure 7 compares the model-simulated ground surface temperature averaged from 20–23 March. Figure 7b demonstrates that in the DARLAM run with the RS mode, the ground surface is, overall, about 1°C warmer after including canopy surface resistance into the surface scheme. This can be explained by the extra resistance to evaporative cooling (besides the aerodynamic resistance in the EB mode) introduced in the pathway of surface water evaporation in the RS mode. Consequently, the surface evaporation is reduced as shown in

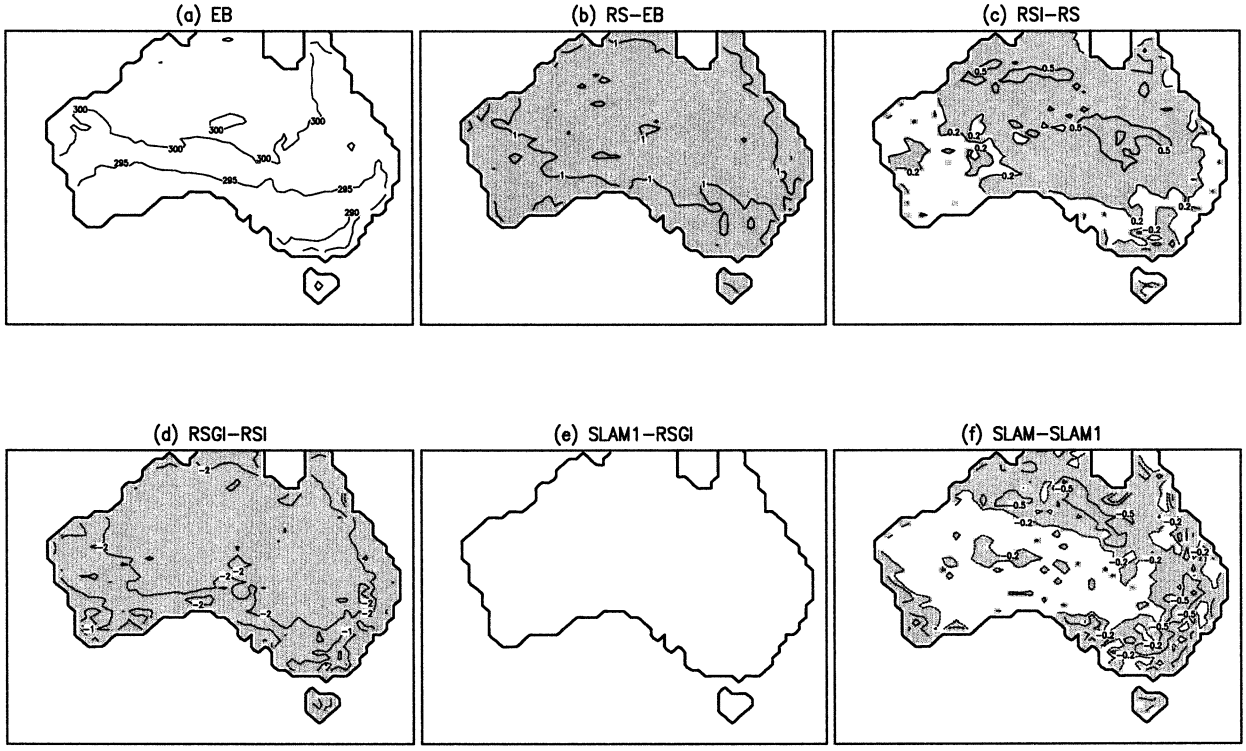

FIG. 7. Comparison of ground surface temperature (K) between six DARLAM runs using different CHASM modes averaged for the period 20–23 Mar. (a) The model simulation using the EB mode; the rest are the difference between simulations from two CHASM modes. Contour intervals are −2, −1, −0.5, and −0.2 K for dashed lines and 0.2, 0.5, 1, 2 K for solid lines. Changes within the range of ±0.2 K are not shown. Changes with magnitude larger than twice the standard deviation derived from the 10 EB perturbation runs are shaded.

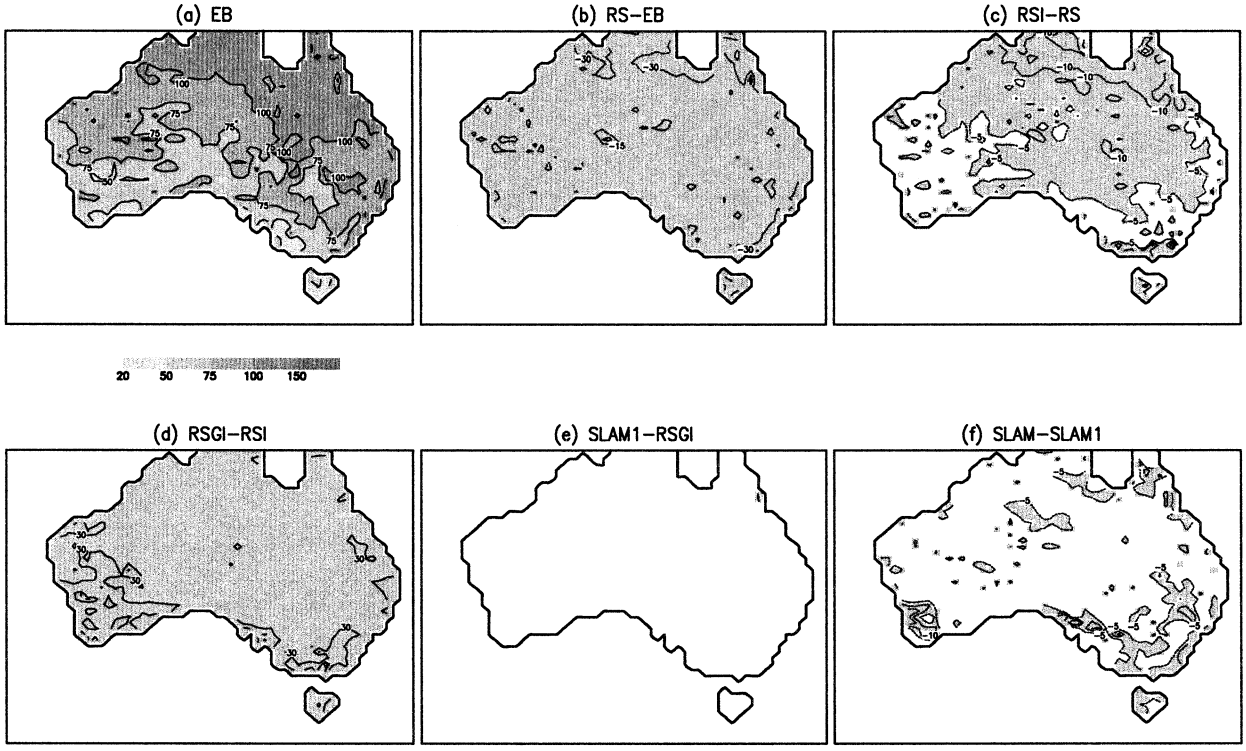

FIG. 8. As in Fig. 7 but for surface evaporation (W m^{-2}). Contour intervals are −30, −15, −10, and −5 W m^{-2} for dashed lines and 5, 10, 15, and 30 W m^{-2} for solid lines. Changes within the range of ±5 W m^{-2} are not shown.

Fig. 8b, resulting in a partition of surface radiative energy into increased surface sensible heat and a warmed land surface. As there is low vegetation coverage over the Australian continent, introducing a canopy interception component in the RSI mode does not alter the model-simulated surface temperature much, with changes of only 0.5°C in the inland region. Figure 8c, however, does indicate some changes in the western and eastern coastal regions where vegetation coverage is high. Large changes in surface temperature are simulated after explicitly parameterizing bare ground evaporation in the RSGI mode. The surface is substantially cooled by about 2°C compared with that in the RSI simulation. Such results are consistent with changes in the surface energy balance in which surface evaporation is significantly increased in the RSGI model by about 30 W m^{-2} (Fig. 8d). Large changes in surface energy balance after explicitly representing bare soil evaporation are also reported in Desborough (1999) and Zhang et al. (2001b), underlining the importance of appropriate treatment of bare soil evaporation in surface parameterizations. Changes of surface temperature and surface evaporation between SLAM1–RSGI and SLAM–SLAM1 are small (Figs. 7e,f and Figs. 8e–g) and only moderate changes are simulated in the coastal regions. Previous studies (e.g., Tuleya 1994) have shown that surface evaporation would affect the model-simulated storm development, including both track and intensity. In agreement with results shown in Fig. 5, for the DARLAM runs with lower surface evaporation by using different CHASM modes (e.g., RS and RSI modes), they also show weaker intensity measured by central MSLP. Such coherence can be explained by the process that surface evaporation is an important moisture source in supporting the storm intensification (Tuleya 1994).

To further demonstrate the short time scale impacts of land surface modeling on the model simulations, we compare the time series of areally averaged surface heat fluxes and ground surface temperatures over a specific location influenced by the low center. Figure 9 shows the results from the model high-frequency outputs (10 times per day) averaged over three land grid boxes near the location of Exmouth (around 22°S and 114°E) as indicated in Fig. 3 where the model shows largest discrepancies. We concentrate on the results from the period 1800 UTC 20 March to 0000 UTC 22 March during which the low pressure center in the model approached the continent in four of the runs (RS, RSGI, SLAM1, and SLAM).

Consistent with results in Figs. 7 and 8, the diurnal variations of the surface energy partition are largely affected by different complexity in CHASM. Significant differences in surface evaporation are simulated (Fig. 9a) during the daytime, with surface evaporation being largely reduced from the EB to RS runs when surface resistance is introduced in the RS mode. Over this particular location, the role of the canopy interception component is also notable. As there is no further resistance

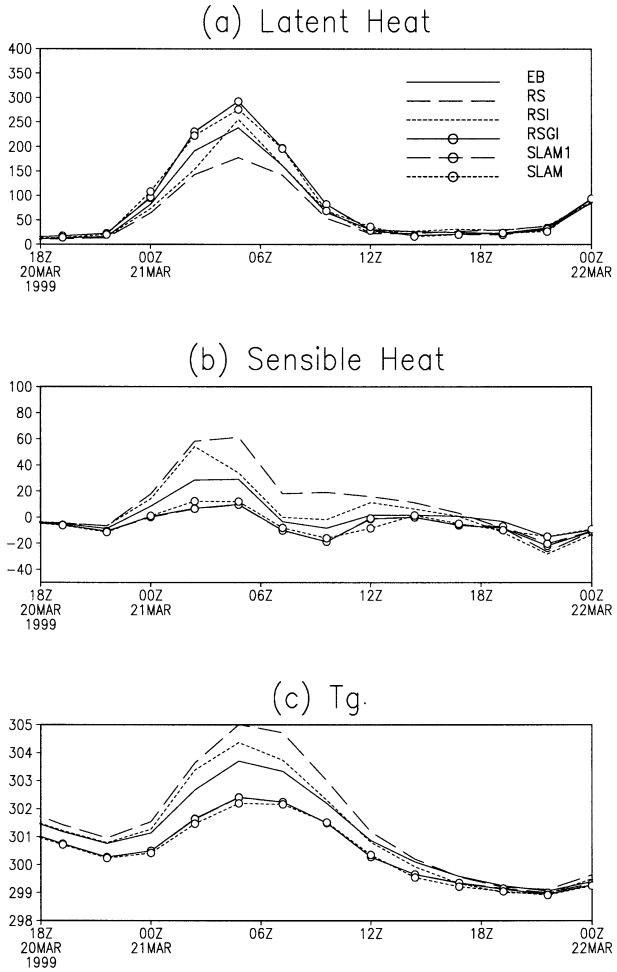

FIG. 9. Time series of DARLAM-simulated surface heat fluxes, surface temperature, and surface zonal wind stress. Results are from the model 10-times-daily outputs, averaged over three model land grid boxes located near Exmouth (around 22°S and 114°E). (a) Latent heat flux (W m^{-2}); (b) sensible heat flux (W m^{-2}); (c) ground temperature (K).

to the evaporation of intercepted water, surface evaporation is increased from the RS to RSI modes after explicitly parameterizing canopy interception. When the bare ground evaporation component is explicitly represented in the RSGI mode, surface evaporation is significantly increased from the RSI mode. This is due to the rapid evaporation process in bare soil without the canopy stomata constraint. However, in this region, there is little differentiation between the RSGI, SLAM1, and SLAM modes, implying very limited contributions from the extra complexities represented in the SLAM1 and SLAM modes in this case.

Constrained by the surface energy balance, with relatively small change in surface radiation (not shown), the surface sensible heat flux (Fig. 9b) shows opposite features to those seen in Fig. 9a. Reduction in surface evaporation in the RS mode leads to a large increase in surface sensible heat fluxes and much warmer surface temperature (Fig. 9c). Explicitly including canopy interception in RSI mode leads to the reduction of surface sensible heat flux and cooler surface temperature. Both surface sensible heat flux and surface temperature respond significantly in the model simulations to the inclusion of a bare-soil evaporation component, with surface temperature being substantially cooler in the RSGI mode. Again, similarities remain between the RSGI, SLAM1, and SLAM modes.

With the influence from different land surface modeling complexity on the surface energy and water partitions (Figs. 8 and 9), it is expected that the model boundary layer processes could be affected and thus lead to impacts on the model simulation of the storm track. To explore the changes of the model boundary processes, here we focus on the analysis of the model's lowest-level wind and air temperature changes between runs from the EB and RS modes (Fig. 10). Changes of the model boundary layer air temperature are primarily attributed to different surface flux calculations, while the changes of low-level wind are the response of model boundary layer circulation to the changes of model boundary layer thermal conditions. The model outputs at three time steps during the period 0200–0700 UTC 21 March are analyzed in Fig. 10, when the low pressure center moves along the coast in the EB run but travels westward in the RS experiment (Fig. 3). We concentrate our analysis during this prelanding period to explore whether continental surface flux anomalies affect the landing process of the low pressure system. It needs to be pointed out that although the horizontal wind change shown in Fig. 10 are not at the system steering level, similar features are seen at other model levels (not shown).

As a common feature seen in Fig. 10, during this period when the low pressure system is over the Indian Ocean, the model shows large differences of low-level air temperature and wind over a large part of the northwest continent. Consistent with the large reduction of surface evaporation in the RS mode (Fig. 8), the model boundary layer is about 0.5°–1°C warmer in the RS mode than in the EB mode. This is because a large part of surface radiative energy is partitioned into surface sensible heat flux, which directly heats the overlying low-level atmosphere. The warmer continent in the RS run (see Figs. 7 and 9c) then leads to an overall cyclonic circulation anomaly, with a reduction in the model sea level pressure over a large part of the continent (not shown). Accordingly, results from the RS experiment show large offshore northward wind anomalies in the costal region and northwestward wind anomalies in the south inland region. This feature is prominent during the whole period examined and it becomes particularly clear at the time of 0710 UTC when the low pressure system moves closer to the continent. The stronger offshore wind anomalies in the RS runs could make a contribution to the further westward movement and a delayed landing of the low pressure system in its sim-

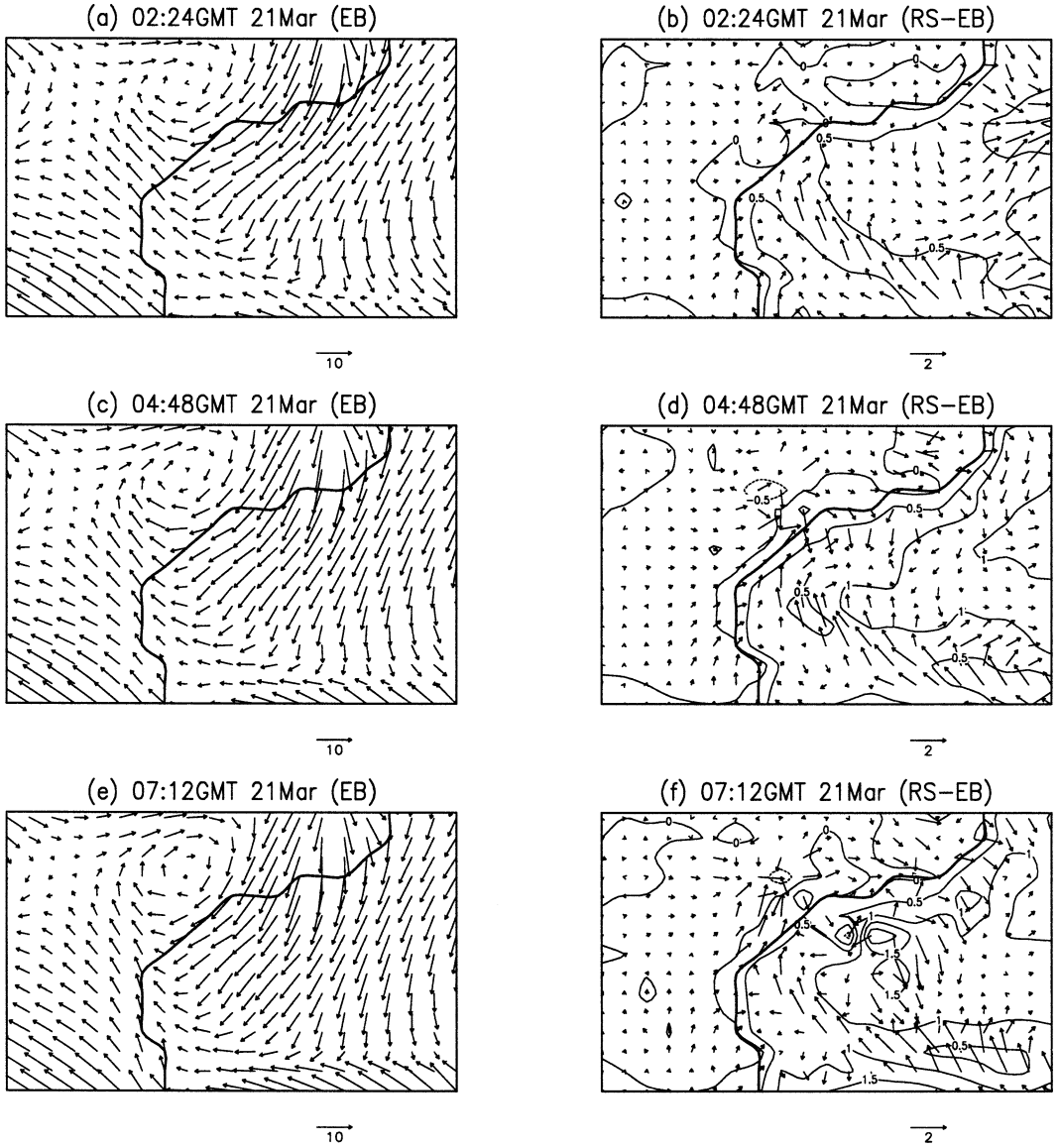

FIG. 10. Comparison of DARLAM-simulated horizontal wind and air temperature at the lowest model level, and difference between EB and RS runs at three time steps during 21 Mar. Arrows represent the changes in low-level horizontal wind and contour lines are the changes of air temperature with the interval level of 0.5 K.

ulation. The large wind anomalies over the region suggest that large-scale circulation in the model can be affected by the model land surface processes, which could in turn affect the motion of the low pressure system embedded in it. Overall, results in Fig. 10 provide a possible explanation of the differences in the low pressure track and its landing time simulated by the EB and RS experiments.

Indeed, there are numerous studies showing how land surface conditions can affect the model simulations and forecasts of tropical cyclones. For instance, Tuleya (1994) studied the sensitivity of a tropical cyclone model to surface boundary conditions and found impacts from surface evaporation and temperature on the storm development and decay in the model. Li et al. (1997) showed the influence of surface sensible heat flux in a high-resolution model study of cyclone landfall. Nevertheless, we must point out results here have only shown the impacts on a low pressure system, which is much weaker in the model than observed. The conclusion from the current study might be somewhat different if the system had been better simulated in terms of its track and intensity. In future research, CHASM will be coupled to a high-resolution tropical cyclone forecasting model to assess the role of land surface modeling on severe tropical cyclone landfall process.

5. On the complexity of land surface schemes and parameter tuning

In section 4, sensitivity to different complexity in representing the land–air interactions is seen in the DARLAM numerical experiments. The model shows its sensitivity in the simulation of the low pressure intensity and movement as well as the associated changes in rainfall, surface temperature, and surface energy partition. One remaining question to be answered is can extra complexity in the surface representation be substituted by surface parameter tuning? Such a philosophy has been applied in the development of land surface models (e.g., Warrilow et al. 1986; McFarlane et al. 1992) in which some parameters in a simple scheme were tuned to try to account for the effects of extra physical processes from the canopy and soil. We revisit the issue here by comparing results from experiments with and without parameter tuning in the CHASM modes.

From the 5-day integration (20–25 March 1999) of the coupled DARLAM experiment with the SLAM mode, as analyzed in section 4, we obtain a set of meteorological forcing data over each land grid point in the model domain. We then run uncoupled offline experiments of CHASM's RS, RSI, RSGI, and SLAM1 modes using the same DARLAM-generated forcing data. As introduced in section 2, surface resistance is the key parameter in the RS, RSI, RSGI, and SLAM1 modes. Thus, we can tune the surface resistance value used in each of the RS, RSI, and RSGI modes to try to match the offline results of the SLAM1 mode, in which the surface resistance value is calculated as a function of temperature, humidity, and radiation. The offline calibration procedure is the same as used in Zhang et al. (2001b). It is performed at each model land grid point by varying the surface resistance value in the range of 10–250 s m^{-1} to achieve the same surface evaporation averages as simulated by the SLAM1 mode over the period of 17–24 March. Following the offline calibration, surface resistance is spatially varying but temporally invariant. After the offline calibration, we then couple the tuned CHASM modes (RS, RSI, RSGI) as well as the SLAM1 mode with DARLAM to rerun the numerical experiments as analyzed in section 4. As the CHASM modes have been tuned to give similar offline simulations of surface energy balance, the differences (if any) seen in the coupled experiments will be due to the effects of physical processes represented by extra complexity in the different modes.

Figure 11 compares the movement of the model-simulated low pressure center from the coupled DARLAM runs with the offline-calibrated RS, RSI, RSGI, and SLAM1 modes. The differences among the four CHASM modes with offline calibration are similar to those seen in Figs. 3 and 4 without any parameter tuning. There are differences in the model-simulated landing positions and tracks, despite the fact that all the surface

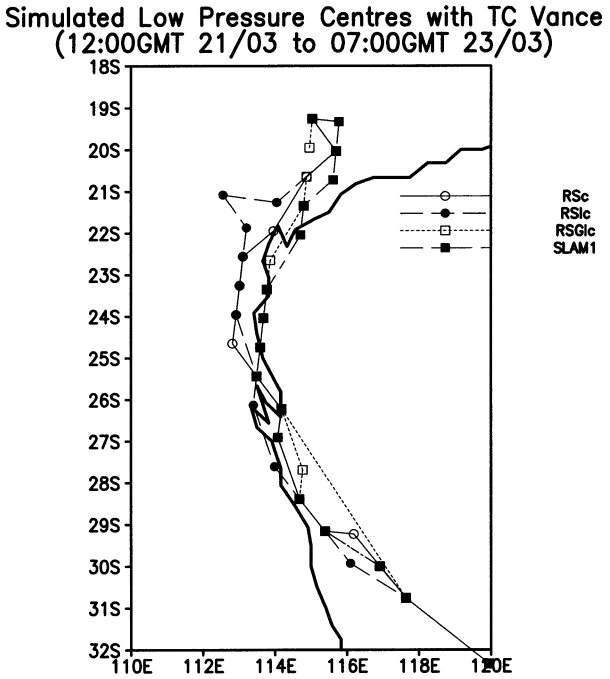

FIG. 11. Comparison of DARLAM-simulated low pressure tracks employing CHASM's RS, RSI, RSGI, and SLAM1 modes after offline calibrations as described in the text.

modes are calibrated to give a similar surface energy balance with the same meteorological forcing.

Similarly, results also show large changes in rainfall location and intensity (Fig. 12). The magnitude and patterns of these changes exhibit similar features to those seen in Fig. 6. The most significant changes are in the RS–EB and RSGI–RSI comparisons. Similarly to the conclusion of Zhang et al. (2001b) for the study of regional climate simulations, the results here demonstrate that the effects from the extra complexity in land surface parameterization cannot be represented by parameter tuning. Adjusting some key parameters in a simple surface parameterization to match the results from complex schemes in the offline experiments cannot guarantee the same model performance in the coupled environment. The experiments here show that explicitly including components of surface resistance and bare ground evaporation can have significant impacts on weather simulations. They should therefore be appropriately parameterized in weather forecast models.

6. Discussion and conclusions

In this paper, we have reported a limited-area model's sensitivity to land surface representation in its simulation of a tropical synoptic event. In particular, we have investigated whether the limited-area model simulations are affected by different complexity modes of a land surface scheme, whether parameterization complexity in land surface representations delivers any prediction

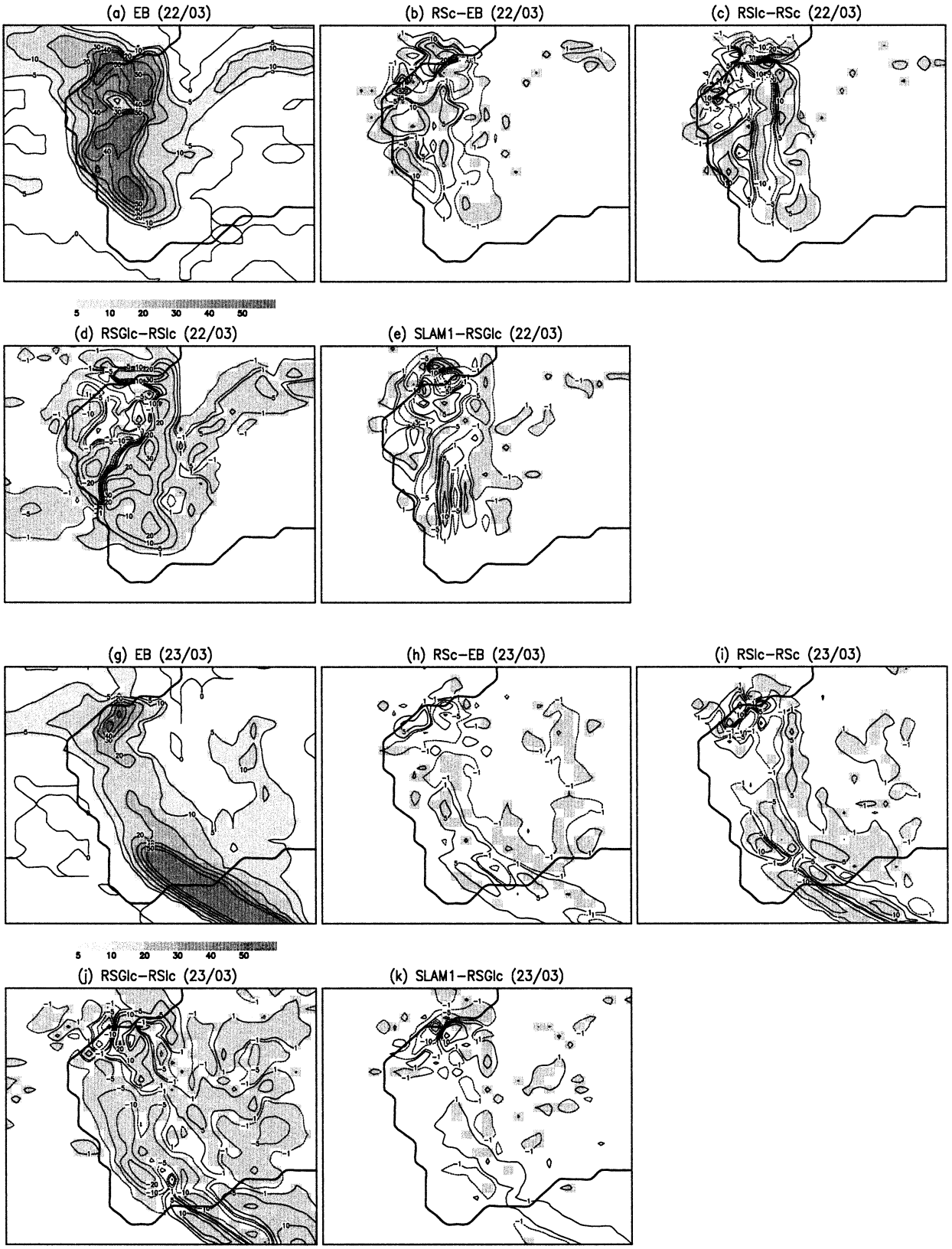

FIG. 12. As in Fig. 6 but for runs following offline calibration of RS, RSI, RSGI, and SLAM1 as described in the text.

benefits, and whether, if so, such complexity can be replaced by parameter tuning.

A multimode land surface scheme CHASM (Desborough 1999) has been coupled to a version of the CSIRO limited-area model DARLAM (McGregor 1987; Walsh and McGregor 1995) with 75-km horizontal and 18-level vertical resolutions. The synoptic event chosen in this case study was a tropical synoptic event associated with the severe Tropical Cyclone Vance. It is emphasized that we are not, here, interested in the verisimilitude of the representation of this tropical cyclone. We made no attempt to contrast the model simulations of the cyclone low pressure center (position and intensity) with observations. Using a relatively low model resolution as well as no synthetic bogusing (e.g., Serrano and Undren 1994; Davidson and Weber 2000) in the model initial condition, we are not in a position to make a detailed comparison with observations. In the analysis of the model results, we have not only concentrated on the model simulations of the positions and intensities of the low pressure center, but also explored the model differences in simulating rainfall and surface temperature during the simulation period.

Comparing the model-simulated tracks of the low pressure center, shows that the overall path of the low center is not strongly affected by using different CHASM modes, primarily due to the well-defined large-scale circulation. However, the local and regional features can be altered. As one measure of the track difference, the simulated landing position of the low pressure center can differ by a number of degrees in latitude and about one degree in longitude. Such differences are larger than the model intrinsic numerical noise from a set of perturbation runs and are comparable with the current errors in operational forecasts (e.g., Davidson and Weber 2001). In addition, the low pressure center landing time is also affected. There can be as large as about 14-h difference. Both the differences of the model-simulated storm track and landing time can be of significant impact on emergency management in the areas affected. There is about 2.5-hPa difference in the model-simulated central pressure, which is larger than the model spread derived from the set of perturbation runs. The reduction of low pressure intensity in two of the model runs is consistent with the reduction of surface evaporation, which is an important part of atmospheric moisture source. Note that the intensity of the low center simulated in the model is significantly weaker than observed and its track is not satisfactorily simulated. Therefore, our results could be somewhat different if the tropical cyclone were properly simulated in DARLAM.

Coupled with different CHASM modes, the model also differs in its simulated distribution and intensity of rainfall. The most significant changes occurred when surface resistance is introduced in the RS mode and when bare ground evaporation is explicitly included in the RSGI mode. Areally averaged rainfall analysis also suggests that the changes in rainfall are not purely due to the displacement caused by the changes in storm track. The RS run has the lowest rainfall amount and the reduction of surface evaporation could be a contributing factor due to the importance of surface water recycling. Changes in surface temperature simulations are consistent with the changes in surface radiative energy partitions. On average, introducing a surface resistance term in the RS mode has warmed the model-simulated surface temperature by about 1°C. This is explained by the reduction of surface evaporation in the RS mode. When surface evaporation is increased in the RSGI mode, it can lead to surface cooling of about 2°C over a large part of the continent. Both Desborough (1999) and Zhang et al. (2001b) reported similar model sensitivity to the treatment of bare ground evaporation in the CHASM modes.

Analysis of areally averaged diurnal variations of surface fluxes and temperature over the location near Exmouth also presents a coherent picture of how surface energy partition and surface temperature are affected by employing different modes. Detailed analysis of the model's lowest-level surface wind changes between the EB and RS runs demonstrated that the enhanced offshore wind anomalies associated with divergent airflow in the RS run could make a contribution to the westward movement of the low pressure center in the RS run. In addition, the land surface process can affect the large-scale circulation in which the low pressure system is embedded and, in turn, affect the track of the low system. Results agree with previous studies that the changes of surface energy partition could induce modification of the low-level boundary processes in the model and therefore affect the model simulations of storm track and intensity (e.g., Tuleya 1994; Li et al. 1997).

In this study, we have also investigated whether aspects of complexity in land surface schemes can be substituted by parameter tuning. Results from our second set of experiments, in which the surface modes are calibrated, underline that some extra complexity to reflect the important processes in the land–air interactions cannot be accounted for by parameter tuning in simple schemes. As found in Zhang et al. (2001b), offline agreement does not ensure that the schemes perform in a similar way when coupled with the host model.

An important conclusion underlined in the research reported here is that the extent of complexity required in the model parameterization depends on the time and spatial scales of the weather and climate phenomena being investigated. For instance, in this study, the importance of bare ground evaporation needs to be addressed because of the dry and sparse vegetation coverage of the Australian continent. In tropical forest regions, the bare-ground component becomes less dominant and other processes such as canopy interception may become important (e.g., Zhang et al. 1996, 2001a; Bowling et al. 2003). In GCM seasonal forecasts, the importance of simulating soil hydrological processes is

realized (e.g., Zhang and Frederiksen 2003). On the other hand, in multidecadal climate simulations and predictions, the importance of incorporating a carbon cycle and interactive vegetation becomes significant (e.g., Cox et al. 2000). The current configuration of the multimodel land surface scheme CHASM is only able to explore the model sensitivity to the complexity in the representation of surface energy balance. The issue of model complexity of representing soil hydrological processes, another important component in land surface modeling needs also to be carefully addressed. A study concerning the relative complexity in modeling surface energy and surface water balances will be pursued in the future.

As discussed throughout the paper, the simulation of the TC Vance is not adequate due to the low resolution of the model, and coarse initial conditions. We emphasize that this study does not allow us to make a solid conclusion on the impacts of land surface parameterization on numerical forecasts of fully developed landfalling tropical cyclones. Results in this study have shown the impacts on the low pressure system simulated in the model associated with TC Vance. Such results have prompted us to conduct ongoing research in which CHASM will be implemented to a high-resolution tropical cyclone forecasting system to answer the questions remaining.

Acknowledgments. This work was initiated when HZ worked at the Australian Nuclear Science & Technology Organisation with AH-S on a one-year leave of absence from BMRC. It forms part of ANSTO's Human Activity and Climate Variability research project. HZ thanks BMRC for support for the ongoing collaboration with ANSTO's HACV project. The authors also acknowledge the constructive comments from Drs. B. Timbal and N. Davidson during the BMRC internal review process and the comments and suggestions from three anonymous reviewers.

REFERENCES

Atkinson, G. D., and C. R. Holliday, 1977: Tropical cyclone minimum sea level pressure/maximum sustained wind relationship for the western North Pacific. *Mon. Wea. Rev.,* **105,** 421–427.

Bowling, L. C., and Coauthors, 2003: Simulation of high-latitude hydrological processes in the Torne–Kalix basin: PILPS Phase 2(e). 1: Experiment description and summary intercomparisons. *Global Planet. Change,* **38,** 1–30.

Cox, P. M., R. A. Betts, C. B. Bunton, R. L. H. Essery, P. R. Rowntree, and J. Smith, 1999: The impact of new land surface physics on the GCM simulation of climate and climate sensitivity. *Climate Dyn.,* **15,** 183–203.

——, ——, C. D. Jones, S. A. Spall, and I. J. Totterdell, 2000: Acceleration of global warming due to carbon-cycle feedbacks in a coupled climate model. *Nature,* **408,** 184–187.

Davidson, N. E., and H. C. Weber, 2000: The BMRC high-resolution tropical cyclone prediction system: TC-LAPS. *Mon. Wea. Rev.,* **128,** 1245–1265.

Davies, H. C., 1976: A lateral boundary formulation for multi-level prediction models. *Quart. J. Roy. Meteor. Soc.,* **102,** 405–418.

Desborough, C. E., 1997: The impact of root-weighting on the response of transpiration to moisture stress in land surface schemes. *Mon. Wea. Rev.,* **125,** 1920–1930.

——, 1999: Surface energy balance complexity in GCM land surface models. *Climate Dyn.,* **15,** 389–403.

Dickinson, R. E., A. Henderson-Sellers, P. J. Kennedy, and M. F. Wilson, 1986: Biosphere–Atmosphere Transfer Scheme (BATS) for the NCAR Community Climate Model. National Center for Atmospheric Research Tech. Note/NCAR/TN-275+STR, Boulder, CO, 69 pp.

Evans, J. L., B. F. Ryan, and J. L. McGregor, 1994: A numerical exploration of the sensitivity of tropical cyclone rainfall intensity to sea surface temperature. *J. Climate,* **7,** 616–623.

Henderson-Sellers, A., 1996: Soil moisture simulation: Achievements of the RICE and PILPS intercomparison workshop and future directions. *Global Planet. Change,* **13,** 99–115.

——, A. J. Pitman, P. K. Love, P. Irannejad, and T. Chen, 1995: The project for intercomparison of land surface parameterization schemes (PILPS): Phase 2 and 3. *Bull. Amer. Meteor. Soc.,* **76,** 489–503.

——, P. Irannejad, K. McGuffie, and A. J. Pitman, 2003: Predicting land surface climates—Better skill or moving targets? *Geophys. Res. Lett.,* **30,** 1777, doi:10.1029/2003GL017387.

Hopkins, L. C., and A. Henderson-Sellers, 1999: PILPS Phase 4b: The impacts of coupled land surface parameterisation schemes to a regional NWP model. Preprints, *14th Conf. on Hydrology,* Dallas, TX, Amer. Meteor. Soc., 328–329.

——, ——, and A. J. Pitman, 1999: Status of the Project for Intercomparison of Land-Surface Parameterization Schemes (PILPS). Preprints, *14th Conf. on Hydrology,* Dallas, TX, Amer. Meteor. Soc., 320–323.

Irannejad, P., A. Henderson-Sellers, and S. Sharmeen, 2003: Importance of land surface parameterization for latent heat simulation in global atmospheric models. *Geophys. Res. Lett.,* **30,** 1904, doi:10.1029/2003GL018044.

Kalnay, E., and Coauthors, 1996: The NCEP/NCAR 40-Year Reanalysis Project. *Bull. Amer. Meteor. Soc.,* **77,** 437–471.

Li, J., N. E. Davidson, G. D. Hess, and G. A. Mills, 1997: A high-resolution prediction study of two typhoons at landfall. *Mon. Wea. Rev.,* **125,** 2856–2878.

Manabe, S., 1969: Climate and the ocean circulation: 1. The atmospheric circulation and the hydrology of the earth's surface. *Mon. Wea. Rev.,* **97,** 739–805.

McFarlane, N. A., G. J. Boer, J.-P. Blanchet, and M. Lazare, 1992: The Canadian Climate Center second-generation general circulation model and its equilibrium climate. *J. Climate,* **5,** 1013–1044.

McGregor, J. L., 1987: Accuracy and initialization of a two-time-level split semi-Lagrangian model. *Short- and Medium-Range Numerical Weather Prediction,* T. Matsuno, Ed., Meteorological Society of Japan, 233–246.

——, K. J. Walsh, and J. J. Katzfey, 1993: Nested modelling for regional climate studies. *Modelling Change in Environmental Systems,* A. J. Jakeman, M. B. Beck, and M. J. McAleer, Eds., John Wiley, 367–386.

McGuffie, K., and H. Zhang, 1997: The tropical cyclone coastal impacts program: A vehicle for coordinated multi-disciplinary research. *Aust. J. Emerg. Manage.,* **12,** 27–30.

Molteni, F., R. Buizza, T. N. Palmer, and T. Petroliagis, 1996: The ECMWF ensemble prediction system: Methodology and validation. *Quart. J. Roy. Meteor. Soc.,* **122,** 73–119.

Nagata, M., and Coauthors, 2001: A mesoscale model intercomparison: A case of explosive development of a tropical cyclone (COMPARE III). *J. Meteor. Soc. Japan,* **79,** 999–1033.

Pitman, A. J., Y. Xia, M. Leplastrier, and A. Henderson-Sellers, 2003: The CHAmeleon Surface Model: Description and use with the PILPS phase 2(e) forcing data. *Global Planet. Change,* **38,** 121–135.

Sampson, C., R. Jeffries, J.-H. Chu, and C. Neumann, 1995: Tropical cyclone intensity. Tropical Cyclone Forecasters Reference

Guide, Naval Research Laboratory Rep. NRL/PU/7541-95-0012, Monterey, CA, 48 pp.
Sellers, P. J., Y. Mintz, Y. C. Sud, and A. Dalcher, 1986: A Simple Biosphere Model (SiB) for use within general circulation models. *J. Atmos. Sci.,* **43,** 505–531.
——, and Coauthors, 1997: Modelling the exchanges of energy, water and carbon between continents and the atmosphere. *Science,* **275,** 502–509.
Serrano, E., and P. Unden, 1994: Evaluation of a tropical cyclone method in data assimilation and forecasting. *Mon. Wea. Rev.,* **122,** 1523–1547.
Shao, Y., and A. Henderson-Sellers, 1996: Validation of soil moisture simulation in landsurface parameterisation schemes with HAPEX data. *Global Planet. Change,* **13,** 11–46.
Timbal, B., and A. Henderson-Sellers, 1998: Intercomparison of land surface parameterizations coupled to a limited area forecast model. *Global Planet. Change,* **19,** 247–260.
Tuleya, R. E., 1994: Tropical storm development and decay: Sensitivity to surface boundary conditions. *Mon. Wea. Rev.,* **122,** 291–304.
Walsh, K., and J. L. McGregor, 1995: January and July climate simulations over the Australian region using a limited-area model. *J. Climate,* **8,** 2387–2403.
——, and I. G. Watterson, 1997: Tropical cyclone-like vortices in a limited area model: Comparison with observed climatology. *J. Climate,* **10,** 2240–2259.
——, and J. J. Katzfey, 2000: The impact of climate change on the polarward movement of tropical cyclone-like vortices in a regional climate model. *J. Climate,* **13,** 1116–1132.
Warrilow, D., A. Sangster, and A. Slingo, 1986: Modelling of land surface processes and their influence on European climate. U.K. Met Office Tech. Rep. 38, 94 pp.
Wood, E. F., and Coauthors, 1998: The Project for Intercomparison of Land Surface Parameterization Schemes (PILPS) Phase 2(c) Red-Arkansas River basin experiment: 1. Experiment description and summary intercomparison. *Global Planet. Change,* **19,** 115–135.
Xia, Y., A. J. Pitman, H. V. Gupta, M. Leplastrier, A. Henderson-Sellers, and L. A. Bastidas, 2002: Calibrating a land surface model of varying complexity using multi-criteria methods and the Cabauw dataset. *J. Hydrometeor.,* **3,** 181–194.
Zhang, H., and C. S. Frederiksen, 2003: Local and nonlocal impacts of soil moisture initialization on AGCM seasonal forecasts: A model sensitivity study. *J. Climate,* **16,** 2117–2137.
——, A. Henderson-Sellers, and K. McGuffie, 1996: Impacts of tropical deforestation. Part I: Process analysis of local climatic change. *J. Climate,* **9,** 1497–1517.
——, ——, and K. McGuffie, 2001a: The compounding effects of tropical deforestation and greenhouse warming on climate. *Climatic Change,* **49,** 309–338.
——, ——, A. J. Pitman, J. L. McGregor, C. E. Desborough, and J. Katzfey, 2001b: Limited-area model sensitivity to the complexity of representation of the land surface energy balance. *J. Climate,* **14,** 3965–3986.